THE ASTROPHYSICAL JOURNAL, 392:320–327, 1992 June 10

THE FATE OF ^{7}Be IN THE SUN

C. W. JOHNSON, E. KOLBE,[1] S. E. KOONIN, AND K. LANGANKE[1]
W. K. Kellogg Radiation Laboratory, California Institute of Technology, Pasadena, CA 91125
Received 1990 August 22; accepted 1991 December 16

ABSTRACT

We reexamine the electron- and proton-capture rates of ^{7}Be important to the solar neutrino "problem." Although the assumptions implied by the traditional Debye approximation for plasma screening are not valid, a careful numerical study changes the electron capture rate by less than 2%. We extrapolate experimental data on the proton capture reaction to astrophysically relevant energies using an energy dependence that includes *d*-wave scattering and is shown to be relatively independent of the model space and interaction used. We find that the solar proton capture rate is lowered by approximately 7% from the currently accepted value.

Subject headings: nuclear reactions, nucleosynthesis, abundances — Sun: abundances

1. INTRODUCTION

The solar neutrino "problem" (see Bahcall & Ulrich 1988 for a review) is still unresolved. Both the Homestake (Davis 1987) and Kamiokande (Hirata et al. 1989) experiments measure a flux of high-energy (above 0.814 and 9.3 MeV, respectively) neutrinos considerably smaller than predicted by the standard solar model. Most of the expected high-energy neutrinos originate from the beta-decay of ^{8}B, which in turn is produced via ^{7}Be$(p, \gamma)^8$B.

In this paper we reexamine the two processes that determine the fate of ^{7}Be in the Sun. This nuclide is consumed by either

$$^7\mathrm{Be} + e^- \rightarrow {}^7\mathrm{Li} + \nu \qquad (1)$$

or

$$^7\mathrm{Be} + p \rightarrow {}^8\mathrm{B} + \gamma\ . \qquad (2)$$

The former has a lifetime in the core of the Sun of $\tau_e \approx 80$ days (depending on temperature and density [Bahcall & Moeller 1969]; this core lifetime is by coincidence approximately the same as the laboratory value) and the latter $\tau_p \approx 200$ yr. Since $\tau_p \gg \tau_e$, the concentration of ^{7}Be is proportional to τ_e, implying that the high-energy neutrino flux is proportional to the product of τ_e and the (p, γ) rate. This latter is of particular interest as it is believed to be the most uncertain nuclear physics input to the solar neutrino problem (Bahcall & Ulrich 1988).

In § 2 we calculate the effect of plasma screening on the bound-electron contribution to the electron-capture rate $\Lambda_e = 1/\tau_e$. Traditionally the Debye-Hückel approximation (DH) was used for the plasma-screened potential for the bound electron. However, there are three assumptions for DH that are weakly violated in the core of the Sun. When the same assumptions are strongly violated in laboratory plasma, experiments show that DH fails dramatically. We have therefore pursued a careful numerical study. We find that, despite these concerns, DH describes the electron capture rate to within 2%.

In § 3 we present the results of a microscopic 3-cluster calculation of the astrophysical *S*-factor for the (p, γ) reaction that takes into account both *d*- and *s*-wave entrance channels; the *d*-waves are unimportant at solar energies but are non-negligible at the energies at which experiments are performed, and thus must be accounted for when extrapolating downward. The energy dependence of the *S*-factor is calculated using two different interactions, and found to be in accord with each other and with previous calculations; the overall scale is then fit to six experimental data sets. Our final conclusion is that the *p*-capture cross-section is approximately 7% lower than the value used in the standard Solar model. Unfortunately, this is still far from resolving the solar neutrino problem.

2. ^{7}Be$(e, \nu)^7$Li

The ^{8}B solar-neutrino flux is inversely proportional to the ^{7}Be electron-capture rate, which in turn is proportional to the density of electrons at the nucleus., $\Lambda_e \propto |\psi_e(0)|^2$. In the laboratory there are only bound electrons, but in the solar plasma continuum electrons contribute as well ($\Lambda_e = \Lambda_{\mathrm{cont}} + \Lambda_{\mathrm{bound}}$) and in fact dominate. In the Sun, $\Lambda_{\mathrm{bound}}/\Lambda_{\mathrm{cont}} \approx 20\%$ (Iben, Kalata, & Schwartz 1967).

The density of electrons at the nucleus is determined by the screened Coulomb potential. The continuum density (and contribution to the rate) is insensitive to screening (Bahcall & Moeller 1969). However, screening is much more important for bound-electron capture, as it reduces the density by about 64% (Iben et al. 1967).

To find the bound electron wave-function ψ_e, one solves the Schrödinger equation

$$\hat{H}\psi_e = \left(-\frac{\hbar^2}{2m_e}\nabla^2 - V\right)\psi_e = E\psi_e\ . \qquad (3)$$

Previously, Iben et al. (1967, hereafter IKS) and others used the DH screened potential (also often referred to as the static screened Coulomb potential), which is found by solving

$$(\nabla^2 - q_{\mathrm{D}}^2)V = -4\pi\rho\ , \qquad (4)$$

where $R_{\mathrm{D}} = 1/q_{\mathrm{D}}$ is the Debye screening length and ρ is the charge density that gives rise to the unscreened potential. If one takes $\rho = \rho_N = Z\delta^3(r)$, one obtains the standard form

$$V_{\mathrm{DH}} = Z \exp(-q_{\mathrm{D}} r)/r\ . \qquad (5)$$

(Here and throughout we take the unit charge $e = 1$.) From this IKS calculated both variational and numerical forms of ψ_e in equation (3). Bahcall & Moeller (1969), like IKS, used V_{DH} in the Schrödinger equation (eq. [3]) to calculate the bound-state

[1] Postal address: Institut für Theoretische, Physik I, Universität Münster Wilhelm Klemm Strasse 9, D-4400 Münster, Germany.

electron wave function; they then use $\rho = \rho_N + \rho_e$ with $\rho_e = -|\psi_e|^2$ in (4) to obtain V_{DH} and use this screened potential in equation (3) to calculate the wave function of *continuum* electrons.

Experiments suggest that the DH potential can fail for bound electrons in plasmas. In particular, Goldsmith, Griem, & Cohen (1984) looked for evidence of line shifts in a laboratory plasma; from the work of Rogers, Graboske, & Harwood (1970), who used the DH potential, one estimates a shift in the Lyman-α line of oxygen of about 0.06 Å, but Goldsmith et al. (1984) found no line shift to within 2 σ uncertainty of 0.02 Å.

This experimental result is not surprising when one considers the assumptions that go into using the DH potential:

1. The mean interparticle spacing $\lambda_m = N_e^{-1/3}$ is much smaller than the Debye length R_D (Landau & Lifshiftz 1980),

$$\lambda_m \ll R_D$$

2. In addition, for applications of a screened potential to bound electrons, the number of plasma electrons within a sphere with the radius of the Bohr orbit must be much larger than 1 (Hummer & Mihalas 1988),

$$N_e(4\pi/3)(a_0/Z)^3 \gg 1 ,$$

or equivalently

$$\lambda_m \ll a_0/Z .$$

3. Finally, using the DH potential assumes that the plasma electrons and ions move on a time scale $1/\omega_{plasma}$ much shorter than the bound electron, so that the plasma "sees" two static point charges (Hummer & Mihalas 1988).

$$\omega_{plasma} \gg \omega_e$$

All three assumptions are strongly violated in the laboratory plasma of Goldsmith et al. (1984), which had an electron density of $N_e = 5 \times 10^{-3}$ Å^{-3} and an electron temperature of $T_e = 0.070$ keV. In the core of the Sun, by way of comparison, $N_e = 60$ Å^{-3} and $T = 1.3$ keV. The assorted scale lengths can be easily computed: for the laboratory experiment, using oxygen ($Z = 8$), one obtains $R_D = 3.1$ Å, $\lambda_m = 6$ Å, and $a_0/Z = 0.07$ Å. For the plasma in the solar core, $R_D = 0.218$ Å, $\lambda_m = 0.255$ Å, and $a_0/Z = 0.133$ Å. Clearly neither assumption (1) or (2) are satisfied in either plasma, although they are more strongly violated in the case of the laboratory experiment.

The time scales are estimated as follows. As the electronic component of the plasma moves the fastest, one estimates $\omega_{plasma} = (4\pi n_0 e^2/m_e)^{1/2}$ (Jackson 1975); and $\omega_e = Z^2e^2/ha_0$. Note that the plasma ions will have a much smaller frequency and longer time scale. In atomic units ($e^2/\hbar a_0 = 1$) one finds that for the laboratory experiment, $\omega_{plasma} = 9.7 \times 10^{-2}$ and $\omega_e = 64$, while for the solar core $\omega_{plasma} = 10$ and $\omega_e = 16$. Thus assumption (3) is also violated, again more strongly for the laboratory experiment.

The failure of the DH potential for laboratory plasmas has been previously addressed by theory. Theimer & Kepple (1970) and Skupsky (1980) accounted for assumption (3) by calculating the bound electron to interact self-consistently with the (still classical) plasma, that is, V_{DH} calculated in equation (2) is calculated using $\rho = Z\delta(r) - |\psi_e(r)|^2$, and then ψ_e calculated in equation (1) using that V_{DH}. Davis & Blaha (1982) then corrected, at least in part, for assumptions (1) and (2) by treating both the free and bound electrons in a self-consistent Hartree calculation with occupation numbers given by a Fermi-Dirac thermal distribution. Exchange and correlation effects for the free electrons were included in an approximate way, but fully antisymmetrized wavefunctions were not used because degeneracy effects were expected to be small for the plasmas in which they were interested (conditions similar to those of the experiments of Goldsmith et al. 1984). All three papers found significant deviations from DH results for laboratory plasmas.

The question arises whether the DH potential fails also for conditions in the solar core, where assumptions (1), (2), and (3) are not quite satisfied. Our detailed numerical calculations, described below, show that in fact DH gives $|\psi_e(0)|^2$ to within a few percent.

Our self-consistent thermal Hartree calculation is similar to that of Davis & Blaha (1982). First, consider the continuum (plasma) electrons. Given a screened electrostatic potential ϕ surrounding a nucleus of charge Z, Schrödinger's equation is integrated to give the continuum electron wavefunctions. The charge density due to the continuum electrons is calculated from these wavefunctions, weighted by the usual thermal Fermi-Dirac distribution, with a chemical potential set to match the average charge density, that is, the electron charge density $-\rho_\infty$ at a large distance from the nucleus Z. In addition, the "hole" in the background (ionized nuclei of charge Z_i) charge distribution is calculated using the distribution $\rho_\infty[1 - \exp(-Z_i\phi/kT)]$. Beyond a certain radius, about $\frac{1}{3}$ to $\frac{1}{2}$ Å, it becomes computationally taxing to sum a sufficient number of partial waves, and we use instead the Thomas-Fermi approximation to arrive at the continuum electron density, an approximation whose validity at large radii we confirmed numerically. We then enforce charge conservation on this charge distribution, so that the integral of the charge density in excess of the average density ρ_∞ is exactly $-Z$, by simply setting the charge density to ρ_∞ beyond an appropriate cutoff radius. This cutoff radius was typically about 1 Å, much larger than both the Debye screening length and the characteristic size of a bound electron orbit, and the discontinuity in density was small. From the excess charge distribution we solved Poisson's equation to obtain the potential screening the nucleus. This process was iterated until convergence.

For a pure plasma (no bound electron), the self-consistent potential was indistinguishable from V_{DH}, independent of the potential used to initiate the iterations. We found that the density of continuum electron calculated in the self-consistent potential (or V_{DH}), is about 2.4% less than that for the density in a pure Coulomb potential. (This is slightly larger than reported by Bahcall & Moeller 1969). This result was not affected by the approximate introduction of exchange forces via the local Slater approximation, $V_{ex}(r) = -3^{1/3}\pi^{-1/3}\rho(r)^{1/3}$.

Next, consider the bound electron. We take the opposite of assumption (3), that the bound electron moves much faster than the plasma electrons. This is not quite true for our conditions, but acts as a limit; and as we shall see, the effect is negligible.

We begin with an analytic treatment in the spirit of Debye-Hückel, which we will call "self-consistent Debye-Hückel" (SCDH). The self-consistent potential V to be used in equation (3) is

$$V = V_N + V_{pN} + V_{pe} . \quad (6)$$

where the first two terms are those of IKS, with $V_N = Z/r$ and V_{pN} solving

$$(\nabla^2 - q_D^2)(V_N + V_{pN}) = -4\pi\rho_N ; \quad (7)$$

that is, $V_N + V_{pN}$ gives V_{DH} (5). The third term is new: V_{pe} is the solution to

$$(\nabla^2 - q_D^2)(V_e + V_{pe}) = -4\pi\rho_e , \tag{8}$$

where V_e is the potential generated by the bare electron,

$$\nabla^2 V_e = -4\pi\rho_e . \tag{9}$$

The total energy of the system can then be written as

$$E = \langle \hat{H} \rangle = T + U_{IKS} + \tfrac{1}{2}U_{pN} + \tfrac{1}{2}U_{pe} \tag{10}$$

where

$$T = \frac{\hbar^2}{2m_e}\int d^3r |\nabla\psi_e|^2 , \tag{11}$$

$$U_{IKS} = \int d^3r \rho_e (V_N + V_{pN}) . \tag{12}$$

$$U_{pN} = \int d^3r \rho_N V_{pN} = -Z^2 q_D ; , \tag{13}$$

$$U_{pe} = \int d^3r \rho_e V_{pe} , \tag{14}$$

where again $\rho_e = -|\psi_e|^2$. The factors of $\frac{1}{2}$ in equation (10) are corrections for self-energy terms of the plasma; one treats the plasma as a dielectric medium and calculates the work necessary to insert the nucleus-electron system into the medium (Jackson 1975). The term $-\frac{1}{2}Z^2 q_D$ is well-known as the interaction energy between the bare nucleus and the plasma; because it is independent of the electron wave function it can be ignored (but will be important later for confirming our results).

An approximate solution to equations (3), (4), and (6) can be obtained with a variational wave function,

$$\psi_e(r) = (\pi a^3)^{-1/2} \exp(-r/a) , \tag{14}$$

where a is chosen to minimize $E = \langle \hat{H} \rangle$. Note for a $^7Be^{+++}$ ion in free space, $a = a_0/4$, where $a_0 = 0.531$ Å is the Bohr radius. Solving the Debye equation (eq. [4]), one obtains

$$V_{pe} = \frac{1}{r}\left[1 - \left(\frac{q_D a}{2}\right)^2\right]^{-2} \times \left[\left[\exp\left(\frac{-2r}{a}\right)\left\{1 + \left[1 - \left(\frac{q_D a}{2}\right)^2\right]\frac{r}{a}\right\} - \exp(-q_D r)\right]\right] + \frac{1}{r}\left[1 - \exp\left(\frac{-2r}{a}\right)\right] - \frac{1}{a}\exp\left(\frac{-2r}{a}\right) . \tag{15}$$

Integrating, one finds the new term in the potential is

$$U_{pe} = -\frac{1}{a}\left[\left[\frac{5}{16} + \frac{1}{2}\left[1 - \left(\frac{q_D a}{2}\right)^2\right]^{-2} \times \left\{\frac{1}{4} - \left(1 + \frac{q_D a}{2}\right)^{-2} + \frac{1}{8}\left[1 - \left(\frac{q_D a}{2}\right)^2\right]\right\}\right] . \tag{16}$$

We can check this result by taking the limit as $q_D a \to 0$, which corresponds to the spatial extent of the bound state becoming small compared to the screening length; i.e., the plasma "sees" a point charge of $Z - 1$. In this limit, equation (16) is $-\frac{1}{2}q_D$. One also has (Iben et al. 1967) $U_{IKS} = -(z/a)(1 + q_D a/2)^{-2}$ so that

$$\lim_{q_D a \to 0} U_{IKS} = -\frac{Z}{a} + Z q_D . \tag{17}$$

The first term of this limit is a self-energy that we discard. Adding the nucleus-plasma interaction energy $-Z^2 q_D/2$, the total potential energy is

$$U = Z q_D - \tfrac{1}{2}Z^2 q_D - \tfrac{1}{2}q_D = -\tfrac{1}{2}(Z-1)^2 q_D , \tag{18}$$

which is exactly what it should be.

In the core of the Sun, $q_D = 4.46$ Å^{-1}, and for our variational wavefunction (14) we find $a_{IKS} = 0.162$ Å, and $a_{sc} = 0.156$ Å. We also solved the system of equations (7)–(10) numerically, and obtained the same "self-consistent Debye-Hückel potential which is V_{DH} plus V_{pe} given in equation (15), although of course the numerical bound-state wavefunction and binding energy differed from that in the variational calculation. One must then fold in the population of bound states in the solar plasma, which is governed by the Boltzmann factor. We follow the recipe of IKS to finally obtain in both the variational and numerical cases

$$\Lambda_{IKS}/\Lambda_{cont} = 1.15 \tag{19}$$

while

$$\Lambda_{sc}/\Lambda_{cont} = 1.17 , \tag{20}$$

a 1.7% difference.

The final step is to treat both continuum and bound electron quantum mechanically (our Hartree calculation, as opposed to DH and SCDH), and it is here that we find a small but definite deviation from a classical (DH) treatment of the plasma.

Our calculation is exactly that of our full self-consistent calculation of the continuum electrons is described above, but with a bound-state electron included. Once again charge conservation is enforced. We find that the self-consistent correction to the DH screening potential in which the bound electron moves is better approximated (though not exactly) by $-1/ZV_{pN}$ than by the V_{pe} given in equation (15). Again, the self-consistent solution is independent of the initial potential used to start the iterations. The density of continuum electrons at the origin is virtually unaffected by the presence of the bound state.

We give our results for a bound electron in Table 1. The units are those of a $^7Be^{+++}$ ion in free space. We compare the numerical results using the DH potential, the self-consistent DH potential (eq. [15]), and the full quantum-mechanical Hartree calculation. Note that one needs not just the binding energy E_b of the electron as calculated in the Schrödinger equation, but also, as in (10), account for the change in the plasma

TABLE 1

NUMERICAL RESULTS FOR BOUND ELECTRON IN $^7Be^{+++}$ AT THE SUN'S CORE

Potential	$\lvert\psi(0)\rvert^2/\lvert\psi_{free}(0)\rvert^2$	E_{bind}/E_{free}	E_{sys}/E_{free}	Rate
DH	0.67	0.22	0.22	18.2%
SCDH	0.72	0.38	0.30	19.9%
Hartree	0.79	0.42	0.34	21.9%

NOTES.—"Free" denotes $^7Be^{+++}$ in free space. The rate is relative to the continuum contribution. See text for details.

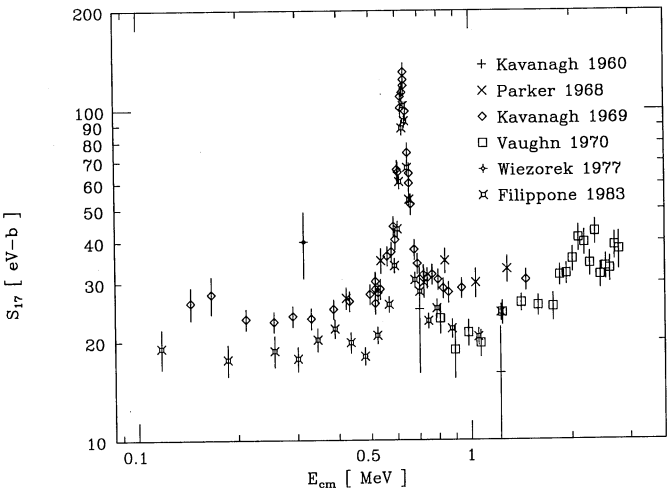

FIG. 1.—World's data on ^{7}Be(p, γ)^{8}B, given as astrophysical S-factor

self energy due to the introduction of the bound electron; the relevant quantity is the "binding energy of the system," E_{sys}. The rate is given in units of the continuum electron rate, and is calculated using the formula of IKS. The full Hartree calculation gives a total electron capture rate 3.7% larger than that using DH; however, subtracting off the 2.4% lowering of the continuum rate by use of DH continuum wavefunctions, the total change in the electron capture rate is only 1.3%—negligible in the context of the solar neutrino problem.

3. ^{7}Be(p, γ)^{8}B

We now turn to the production of ^{8}B via the (p, γ) reaction. There have been six measurements of the ^{7}Be(p, γ)^{8}B cross section, shown in Figure 1: Kavanagh (1960), Parker (1966, 1968), Kavanagh et al. (1969), Vaughn et al. (1970), Wiezorek et al. (1977), and Filippone et al. (1983). The lowest experimental data point is at center-of-mass $E = 117$ keV; to determine the reaction rate in the solar core, the data must be extrapolated to lower energies ($E \approx 0$–20 keV) using an energy dependence calculated in a direct-capture model.

There are three sources of uncertainty to be considered: uncertainty in the theoretical energy dependence (which in turn depends on the model space and interaction used), uncertainty in the one-parameter (overall normalization) fit to the experimental data, and uncertainty in the normalization of the experimental data. We consider only the first two in this paper. Barker & Spear (1986) have raised some questions about the third, noting that many experimental normalizations can be traced to a stopping power of protons in lithium that Barker & Spear (1986) consider suspect. However, we note that Filippone et al. (1983) found no change within their quoted uncertainties if their data were normalized in a manner independent of this stopping power.

The standard solar model (Bahcall & Ulrich 1988) currently assigns to the ^{7}Be(p, γ)^{8}B reaction a zero-energy S-factor of $S_{17}(E = 0) = 0.0243 \pm 0.018$ keV barn^{-1} (the uncertainty is that of Parker 1986; Bahcall & Ulrich 1988 quote a 3 σ uncertainty, which is 22%) and an energy derivative of $S'_{17}(0) = -3 \times 10^{-5}$ barns. These values have been obtained from extrapolations that use the energy dependence of a potential model of structureless ^{7}Be + p fragments and consider only s-wave scattering in the entrance channel (Tombrello 1965).

Robertson (1973), and later Barker (1980) and others, criticized this extrapolation, pointing out that d-wave capture cannot be neglected at the energies where the data are taken ($E \leq 1$ MeV). These authors showed that d-wave capture modifies the energy dependence of the low-energy cross section to the extent that the extrapolated value of $S_{17}(0)$ is reduced by about 15%. One weakness in this analysis is that there are essentially no experimental constraints on the d-wave potential. Barker found only a slight dependence on the d-wave depth and so equated the d-wave and s-wave interactions, the parameters of the latter being determined by the experimental ^{7}Li + n scattering and capture cross sections. While Filippone et al. (1983) adopted an extrapolated $S_{17}(0)$ using only s-wave capture (Tombrello 1965), they noted that use of Barker's (1980) energy dependence gave an extrapolated value 10%–15% lower.

Two recent microscopic calculations of the ^{7}Be(p, γ)^{8}B reaction have treated the various s- and d-wave capture contributions consistently within the same 8-nucleon model space (Descouvemont & Baye 1988; Kolbe, Langanke, & Assenbaum 1988). While these approaches, which use an effective nucleon-nucleon interaction, are not accurate enough to predict absolute cross sections, the calculated energy dependences agree qualitatively with that of Barker (1980) and so confirm the importance of d-wave capture contributions. However, neither work extrapolated the experimental data to low energies using the calculated energy dependence.

3.1. *Microscopic Calculation of the Energy Dependence*

In this section, we present microscopic calculations that extend the approach of Kolbe et al. (1988) to a full dynamical 3-cluster treatment of the reaction. In detail, our model space is spanned by fully antisymmetric p + ^{3}He + ^{4}He cluster wave functions

$$|\Psi^{J\pi}\rangle = \mathscr{A}\left\{\sum_I [(\Phi^{I_1}_{\rm Be} \otimes \Phi^{I_2}_p)^I \otimes Y_l(\hat{r})]^{J\pi} g^{J\pi}_{l,I}(r)\right\} \quad (21)$$

with

$$|\Phi^{I_1}_{\rm Be}\rangle = \mathscr{A}\{\Phi_\alpha[\Phi^{I'}_{\rm He} \otimes Y_L(\hat{r}')]^{I_1} \tilde{g}^{j\pi}_{L,I}(r')\} \; . \quad (22)$$

Here, we have formally written the 8-nucleon wave function as a ^{7}Be + p cluster function, while the internal degrees of freedom of the ^{7}Be fragment are described by a ^{3}He + α cluster function. In equation (21), $\Phi^{I_2}_p$ is the spin-isospin function of the proton (spin $I_2 = \frac{1}{2}$), while in equation (22), Φ_α and $\Phi^{I'}_{\rm He}$ describe the internal degrees of freedom of the α particle (assumed to be $T = S = 0$) and of the ^{3}He-nucleus ($I' = \frac{1}{2}$). The separations of the p + ^{7}Be and ^{3}He + ^{4}He clusters are $\boldsymbol{r}$ and $\boldsymbol{r}'$, respectively. Correspondingly, $g(r)$ and $\tilde{g}(r)$ are the relative wave functions between these cluster fragmentations; they might be different for different values of the channel spin I. Thus, the relative wave function $\tilde{g}(r')$ in equation (22) carries an index I. Further, as we will in the following consider only the ground-state of ^{7}Be, $L = 1$ and $I_1 = 3/2$, so that the channel spin I in equation (21) can thus take the values $I = 1$, 2. To reduce the computational effort, we have neglected coupling of channels with different orbital angular momenta. Thus, $l = 1$ for the ^{8}B ground state, while $l = 0$, 2 for the important ^{7}Be + p scattering states, allowing $E1$ capture into the ^{8}B ground state.

Our calculations use either the Minnesota force (Chwieroth et al. 1973) or the Hasegawa-Nagata force (Furitani et al. 1980) as the effective nucleon-nucleon interaction. We have adjusted

one of the parameters in each of these interactions (the exchange mixture parameter u in the Minnesota force and the Majorana exchange parameter m of the medium-ranged Gaussian in the force of Furitani et al. 1980) to reproduce the binding energy of the ^{8}B ground state relative to the ^{7}Be + p threshold. The properties of the individual clusters (p, ^{3}He, ^{4}He) do not depend on these interaction parameters.

We determine the dynamical degrees of freedom in our approach—the relative wave functions g and $\tilde{g}$ in equations (21), 22)—by solving the many-body Schrödinger equation assuming fixed internal cluster structures. Different procedures for doing so have been used for the bound and scattering states. In both cases we first calculate the ^{7}Be ground state by a standard two-cluster RGM treatment of the seven-nucleon problem, equation (22). To reduce the numerical effort necessary to calculate the ^{8}B wave functions, we have then expanded the radial wave function $\tilde{g}$ in a minimal number of basis wave functions. As in Kolbe et al. (1988), we succeeded in representing $\tilde{g}$ by a sum of only two radial harmonic oscillator states $u_N^L(r, \beta)$ with different width parameters β and quantum numbers ($L = 1, N = 2n + L = 1$)

$$\tilde{g}_{L=1}^{J^\pi, I}(r) = \alpha_1 u_{N=1}^{L=1}(r, \beta_1) + \alpha_2 u_{N=1}^{L=1}(r, \beta_2) . \quad (23)$$

When inserted in equation (22), this expression well-reproduces the properties of the ^{7}Be ground state obtained in the full RGM approach.

In solving the 3-cluster problem, we have expanded the relative wave function $g_{lI}^{J^\pi}$ in a basis of 24 harmonic oscillator states $u_N^l(r, \gamma)$:

$$g_{l,I}^{J^\pi}(r) = \sum_{m=1}^{6} \sum_{n=0}^{3} \beta_{m,n}^{J^\pi I} u_{N=l+2n}^{l}(r, \gamma_m) . \quad (24)$$

At a radius beyond the range of the nuclear forces and the influence of the Pauli principle, $g_{lI}^{J^\pi}$ is matched to the appropriate asymptotic boundary condition for bound and scattering states, respectively.

In our bound state calculation, we have allowed the parameters α_i and $\beta_{m,n}^{J^\pi I}$ in equations (23) and (24) to vary, particularly allowing α_1, α_2 to be different for any triplet of indices (m, n, I). The values of these parameters were determined by minimizing the ^{8}B ground state energy. If we adopt $u = 1.1315$ in the Minnesota force and $m = 0.3714$ in the Hasegawa-Nagata force, our approach can reproduce the experimental binding energy of the ^{8}B ground state relative to the p + ^{7}Be threshold ($E_B = 138$ keV). These values of (u, m) are typical for studies of light nuclear reactions.

For our two different effective interactions, the parameters in the ^{7}Be ground state (22) are

$$\alpha_1 = \quad 0.01390 \quad \beta_1 = 2.319 \text{ fm}$$

$$\alpha_2 = -0.03334 \quad \beta_2 = 1.026 \text{ fm}$$

for the Minnesota force and

$$\alpha_1 = \quad 0.01229 \quad \beta_1 = 2.331 \text{ fm}$$

$$\alpha_2 = -0.06986 \quad \beta_2 = 1.046 \text{ fm}$$

for the Hasegawa-Nagata force.

For the scattering states, we solved the 3-cluster problem by introducing a set of ^{7}Be pseudostates. These are obtained by diagonalizing the microscopic seven-nucleon Hamiltonian in the two-dimensional Hilbert space spanned by the basis functions (eq. [22]) considering the coefficients α_1, α_2 as variables and using the same width parameters as above. The resulting lower eigenstate is identical to the ^{7}Be ground state defined above. The upper pseudostate generally does not correspond to a physical level, but rather is just a tractable way of accounting for distortion in the scattering states (Shen et al. 1985). Upon inserting the two ^{7}Be configurations into equation (21), we define p + ^{7}Be channels, which, after the appropriate asymptotic boundary condition is imposed, can be interpreted as the (physical) p + ^{7}Be system and an inelastic p + ^{7}Be* channel. Note that the inelastic channel is closed at the low p + ^{7}Be energies of interest in this paper. The corresponding coupled-channel problem can be solved with standard techniques (Wildermuth & Tang 1977).

At low energies, the ^{7}Be(p, γ)^{8}B cross section is dominated by $E1$ capture into the ^{8}B ground state. We have calculated the respective many-body matrix elements of the electric dipole operator in the long-wavelength approximation, truncating the integral over the radial relative coordinate at 200 fm.

It is convenient to present the cross section in terms of the astrophysical S-factor:

$$S(E) = \sigma(E)E \exp\{2\pi\eta(E)\} , \quad (25)$$

where in the present case the Sommerfeld parameter is given by $2\pi\eta(E) = 117.47/\sqrt{E}$ with the energy expressed in keV. Furthermore, for applications to the solar neutrino problem, the relevant quantities are $S(0)$ and its first two derivatives at $E = 0$. For these latter two we use the normalization-independent parameterization given by Williams & Koonin (1981), namely

$$\frac{1}{S}\frac{dS}{dE} = a + bE .$$

These three quantities are given in Table 2. We give the theoretical $S_{17}(0)$ only for completeness; in the next subsection, we use experiment to set the overall normalization. While the Minnesota force predicts an S-factor 5% smaller than that of the Hasegawa-Nagata force, the two calculations predict nearly identical energy dependences for the low-energy cross section. Therefore we adopt values of $a = -1.00$ MeV^{-1} and $b = 8.96$ MeV^{-2} with "theoretical uncertainties" of 1% or less.

Our calculations with the Hasegawa-Nagata force can be compared with those of Kolbe et al. (1988), who adopted the same effective interaction but a less flexible model space. Our cross sections are about 10% lower than those of Kolbe et al. (1988) because of a smaller amplitude in the asymptotic ^{8}B ground state. The calculated energy dependences are similar, as are the relative contributions of $E1$ capture from the

TABLE 2

LOW-ENERGY PARAMETERS OF COUPLED-CLUSTER CALCULATION OF S_{17}

Parameter	Minnesota	Hasegawa-Nagata
$S(0)$ (keV) barn^{-1}	0.02514	0.02384
a (MeV^{-1})	−0.99	−1.01
b (MeV^{-2})	9.01	8.90

NOTES.—a and b are from the parameterization of Williams & Koonin 1981; see text.

$p + {}^7$Be d-wave. Distortion effects are important in the ^{8}B ground state, but negligible in the low-energy ^{7}Be + p scattering states.

Barker adjusted his parameters for his model using ^{7}Li(n, γ)^{8}Li; therefore, for comparison, we have calculated the ^{7}Li(n, γ)^{8}Li capture cross sections into the ^{8}Li ground state using the Hasegawa-Nagata force. The calculation is identical to that for ^{7}Be(p, γ)^{8}B, except for the appropriate changes in the isospin quantum numbers and in the internal cluster parameters for the ^{3}H and ^{7}Li nuclei. To reproduce the binding energy of ^{8}Li, we have adjusted the Majorana exchange parameter in the effective interaction to $m = 0.3684$. With a flux of neutrons with a (center-of-mass energy) Maxwell-Boltzmann distribution with $kT = 21.3$ keV (which corresponds to a distribution of laboratory energies with $kT = 25$ keV), we find a capture cross section of 30.6 mbarns. This should be compared to the experimental values of 40.2 ± 2 mbarns (Imhof et al. 1959) and 45.4 ± 3.0 mbarns (Lynn, Jurney, & Raman 1991) which have been derived by scaling by $1/v$ and by adopting the experimental branching ratio for capture into the excited 1^+ state ($10.6 \pm 10\%$) of ^{8}Li as we calculate only capture to the ground state. Note, however, that our present results should not be overinterpreted as our calculation does not reproduce the scattering length a_2 in the $I = 2$ ^{7}Li + n channel, which, in turn, yields the dominant contribution (91%) to the low-energy capture cross section. We find $a_2 = 0.26$ fm, while the experimental value is -3.59 ± 0.06 fm. On the other hand, we find a good agreement in the $I = 1$ channel: $a_1 = 1.25$ fm, to be compared with the experimental value 1.09 ± 0.2 fm.

We argue, however, that our results for the ^{7}Li(n, γ)^{8}Li reaction do not really bear on the quality of our ^{7}Be(p, γ)^{8}B results. The ^{7}Li(n, γ)^{8}Li reaction is sensitive to the complete (i.e., interior) wave functions in the initial and final channels, as penetration of the neutron is not inhibited by the Coulomb barrier. In contrast, the ^{7}Be(p, γ)^{8}B reaction at low energies is a direct capture process sensitive mainly to the asymptotic forms of the wave functions, especially to the amplitudes of the Whittaker functions of the ^{8}B ground state and to the s- and d-wave phase shifts. The latter dominate the energy dependence of the low-energy cross section, while the spectroscopic amplitude determines its absolute magnitude.

3.2. *Extrapolation of Experimental Data*

Our most important results are the energy dependences and the subsequent extrapolations to $E = 0$. Not only do our calculated energy dependences with two different effective interactions agree well with each other, but they are also in good agreement with the microscopic GCM calculation of Descouvemont & Baye (1988) (who used a somewhat less flexible microscopic 3-cluster approach and yet a third effective interaction), and the phenomenological potential model results of Barker (1980). We can therefore conclude that the energy dependence of the low-energy ^{7}Be(p, γ)^{8}B cross section as calculated in all of these approaches are reasonable and that they differ from the experimental data only by a normalization factor (as can be embodied in the proton spectroscopic factor of ^{8}B).

It is important to note that these calculations can only be trusted for $E < 430$ keV, above which the inelastic excitation of the $1/2^-$ state in ^{7}Be is possible, and that no calculation to date includes this inelastic channel. Because flux is lost to this channel, optical-potential models (Tombrello 1965 or Barker 1980) should use a complex, not real, potential above 430 keV. As noted above, our 3-cluster model only includes $3/2^-$ states and so also does not describe this inelastic channel; an extension of the present microscopic calculation is in principle straightforward, but computationally very taxing. The loss of flux could be nonnegligible: the isospin-conjugate reaction, ^{7}Li(n, n')^{7}Li, shows an abrupt rise from threshold in the excitation function for 480 keV photons (Ajzenberg-Selove 1984). For this reason we only use our calculation of the ^{7}Be(p, γ)^{8}B reaction at energies where the inelastic channel is not open.

In view of the foregoing, we are justified in using our energy dependence, consistently including the s- and d-wave capture contributions, to extrapolate the experimental low-energy data below 430 keV to $E = 0$, with the normalization constant determined by a least-squares fit. Only the data of Kavanagh et al. (1969) (hereafter Kav69), Wiezorek et al. (1977), and Filippone et al. (1983, hereafter Fil83) allow this procedure. [In fact, Parker 1968 has one point at $E_{\rm c.m.} = 422$ keV; however, one obtains the same result by either (a) normalizing our theoretical curves by the single point at 422 keV or (b) normalizing Kav69 and Fil83 as described below.] Figure 2 shows the fits to Kav69 and Fil83.

However the remaining three experiments (Kavanagh 1960; Parker 1966, 1968; Vaughn et al. 1970) provide valuable information and should not be excluded. The experiments of Kav69 and Fil83 include data both below and above 430 keV. Therefore we normalized the high-energy data of Kav69 and Fil83 to match the experiments of Kavanagh (1960), Parker (1966, 1968), and Vaughn et al. (1970). (We only used the Kav69 data, which is plotted in Kavanagh 1972, up to 1460 keV.) This normalization is then automatically extrapolated to $E = 0$ by the low-energy fit to Kav69 and Fil83. This procedure not only avoids the use of suspect theoretical calculations above 430 keV, but also obviates the need to carefully subtract the resonance at 630 keV (below 430 keV the resonance contributes no more than 3% to the cross section). The extrapolated values of S_{17} of Kavanagh (1960), Parker (1968), and Vaughn et al.

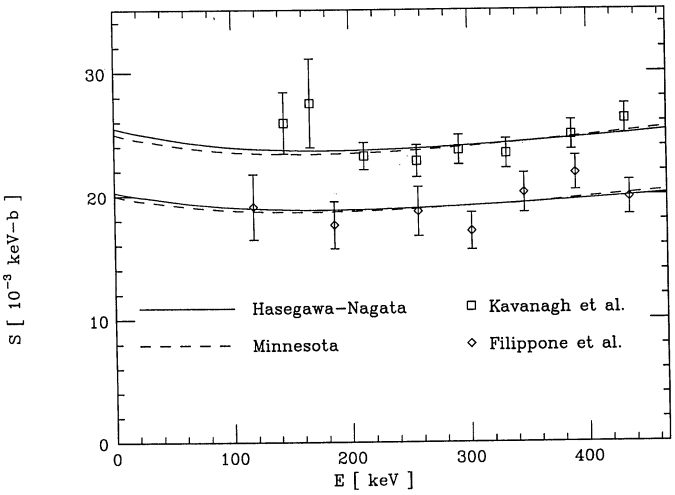

FIG. 2.—Extrapolation of S_{17} to zero energy. Upper data set is from Kavanagh et al. (1969); lower is from Filippone et al. (1983). The solid lines are calculated using the Hasegawa-Nagata interaction; the dashed lines are calculated using the Minnesota interaction. The error bars do not include the systematic error from uncertainty in σ_{dp}.

TABLE 3

EXTRAPOLATION OF EXPERIMENTAL S-FACTOR TO $E = 0$

EXPERIMENT	$S_{17}(0)$ (eV bar^{-1}) Previous[a]	Present
Kav 60	16 ± 6	15 ± 6
Par 68	28 ± 3	27 ± 4
Kav 69	27.3 ± 2.4	25.2 ± 2.4
Vau 70	21.4 ± 2.2	19.4 ± 2.8
Wie 77	45 ± 11	41.5 ± 9.3
Fil 183	22.2 ± 2.8	20.2 ± 2.3

[a] From Filippone 1986; Parker 1986.

(1970) using either Kav69 or Fil83 for the three "high-energy" experiments were consistent within 4%, 3%, and 7%, respectively.

Before presenting our results, we comment on the normalization of the data. Most of the experimental cross-sections were normalized using the broad 0.77 MeV resonance in ^{7}Li(d, p)^{8}Li. The measured value of σ_{dp} range from 138 to 211 mbarns (see Filippone 1986). We use the currently adopted value of 157 ± 10 mbarns.

Another method of normalization is via direct measurement of ^{7}Be activity. Wiezorek et al. (1977) used only this method. Note that while the extrapolated value from their experiment, which measured the (p, γ) cross-section at only energy, is nearly twice that of all other experiments, because of the large error bars this experiment has a nearly negligible effect on our results. Filippone et al. (1983) used both σ_{dp} and ^{7}Be activity to normalize their cross-sections and found consistent results within their uncertainties. Following Parker (1986) we normalize Fil83, and the remaining four experiments, with $\sigma_{dp} = 157 \pm 10$ mbars.

In Table 3 we give our extrapolated values of $S_{17}(0)$ for each of the six experiments, as well as the previously adopted extrapolations (Filippone 1986; Parker 1986). The "theoretical uncertainty," that is, the difference between using the energy-dependence calculated using the Minnesota or Hasegawa-Nagata force, was less than 2%. Our new values were consistently lower than those of previous extrapolations by up to 10%. (The extrapolated value of Kavanagh [1960] did not change, but this is likely due to rounding off to two digits.)

The six experimental values of $S_{17}(0)$ in Table 3 were averaged in two different ways, both of which gave the same result of 0.0224 keV barn^{-1}. The first was a simple weighted average. The combined uncertainty is then calculated as 0.0013 keV barn^{-1}. However, $\chi^2/(N-1)$, where the number of experiments, N, is 2.1, implying that the error bars on some or all of the experiments were underestimated. Following accepted practice (see, e.g., section IV.C.2 of Particle Data Group 1990), we multiply σ by $\sqrt{\chi^2/(N-1)}$ and obtain an uncertainty of $\sigma = 0.0019$ keV barn^{-1}.

This analysis ignores the fact that all but one experiment was normalized by $\sigma_{dp} = 157 \pm 10$ mbarns; this contribution to the uncertainty should be treated as an overall systematic uncertainty and should not be used while averaging the experiments. For our second analysis we ignored the experiment of Wiezorek et al. (1977), which was normalized by ^{7}Be activity, and performed a weighted average of the remaining five experiments, using, however, uncertainties calculated without $\Delta\sigma_{dp}$. The result was 0.0224 ± 0.0010 keV bar with $\chi^2 = 8.5$; multiplying the uncertainty by $\sqrt{\chi^2/N-1}$ yields 0.0016 which *then* is combined, in quadrature, with the 6.4% "systematic" uncertainty in σ_{dp} to obtain 0.0021. We adopt this latter, more conservative uncertainty.

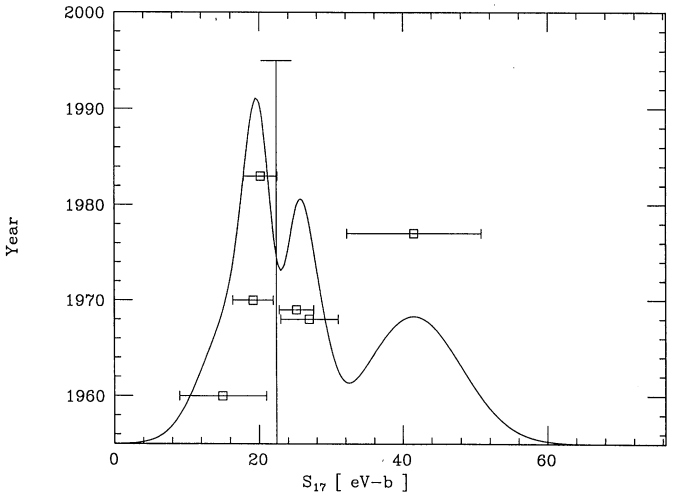

FIG. 3.—Ideogram of the extrapolated measurements of $S_{17}(0)$. Each experiment is represented by a Gaussian with width σ (shown also as the error bars) and with area proportional to $1/\sigma$. Vertical line is adopted value of $S_{17} = 22.4$ eV barn^{-1}.

To illustrate the uncertainties, we present in Figure 3 an ideogram of the values of $S_{17}(0)$ extrapolated from each experiment, expressed as a Gaussian with width σ and total area proportional to $1/\sigma$ (see Particle Data Group 1990).

In summary, then, our final result is $S_{17}(0) = 0.0224 \pm 0.0021$ barn^{-1}. This corresponds to a 3 σ uncertainty of 28%. The "theoretical uncertainty" we have argued is quite small, and we believe that our quoted uncertainty accurately reflects uncertainties in the experiments themselves as well as uncertainty in σ_{dp}.

Some authors have advocated even lower values of S_{17}. Turck-Chieze et al. (1988) adopt a value of 0.0209 keV barn^{-1}, by reducing the previously adopted value of S_{17} by 15% to adjust for d-wave capture, following a statement of Filippone et al. (1983) that inclusion of d-wave capture reduces S_{17} by 10%–15%. We find inclusion of d-wave capture only reduces extrapolated S_{17} by 10% or less. Barker & Spear (1986) propose a greater reduction in $S_{17}(0)$ to 0.017 keV barn^{-1}. They discard Kavanagh et al. (1969) and Parker (1968), include d-wave capture, and finally advocate a significantly lower value of σ_{dp}. While one might exclude the experiment of Wiezorek et al. (1977) as being spurious—and we in fact found it made no difference in the final result—clearly Parker (1968) and Kavanagh et al. (1969) are consistent with each other and should not be excluded. For reasons discussed in the second paragraph of this section, we do not use a lower σ_{dp}.

4. CONCLUSION

We have reexamined the two nuclear processes determining the fate of ^{7}Be (and hence the production of ^{8}B) in the Sun. For the dominant electron capture reaction that makes ^{7}Be unavailable for transmutation into ^{8}B, we have carefully reconsidered the approximations that go into computing the electron density and performed a self-consistent, thermal Hartree

calculation. The net increase in the solar rate for this process relative to previous calculations is small. For the proton-capture reaction, which produces the ^{8}B and thus the high-energy neutrinos seen (or rather not seen!) in terrestrial detectors, we have performed a microscopic cluster calculation of the energy dependence of the astrophysical S-factor that includes capture from d-waves. Our extrapolations of the experimental data using all six experiments decreases the proton capture rate, and hence the ^{8}B neutrino flux, is from the currently accepted value by about 7%. While not insignificant, this reduction is still far from explaining the solar neutrino "problem."

We thank C. Carraro for a helpful discussion of the material in § 2, and J. N. Bahcall, F. C. Barker, B. W. Filippone, and R. W. Kavanagh for comments and helpful suggestions on § 3; in particular we thank B. W. F. and R. W. K. for providing the statistical and systematic uncertainties in their measurements. This work was supported in part by the National Science Foundation grants PHY86-04197 and PHY88-17296.

REFERENCES

Ajzenberg-Selove, F. 1984, Nucl. Phys. A, 413, 1
Bahcall, J. N., & Moeller, C. P. 1969, ApJ, 155, 511
Bahcall, J. N., & Ulrich, R. K. 1988, Rev. Mod. Phys., 60, 297
Barker, F. C. 1980, Australian J. Phys., 33, 177
Barker, F. C., & Spear, R. H. 1986, ApJ, 307, 847
Chwieroth, F. S., Brown, R. E., Tang, Y. C., & Thompson, D. R. 1973, Phys. Rev. C, 8, 938
Davis, J., & Blaha, M. 1982, J. Quant. Spectros. Rad. Trans., 27, 307
Davis, R. 1987, in Proceedings of the Seventh Workshop On Ground Unification, Toyama, Japan 1986, ed. J. Arafune (Singapore: World Scientific), 237; Rowley, J. K., Cleveland, B. T., & Davis, R. 1984, in AIP Conf. Proc. No. 126, Solar Neutrinos and Neutrino Astronomy, ed. M. L. Cherry, K. Lande & W. A. Fowler (New York: AIP), 1
Descouvemont, P., & Baye, D. 1988, Nucl. Phys. A, 487, 420
Filippone, B. W. 1986, Annu. Rev. Nucl. Sci., 36, 717
Filippone, B. W., Elwyn, A. J., Davids, C. N., & Koetke, D. D. 1983, Phys. Rev. Lett., 50, 412; Phys. Rev. C, 28, 2222 (Fil83)
Furutani, H., Kanada, H., Kaneko, T., & Nagata, S. 1980, Prog. Theor. Phys. Suppl., 68, 215
Goldsmith, S., Griem, H. R., & Cohen, L. 1984, Phys. Rev. A, 30, 2775
Hirata, K. S., et al. 1989, Phys. Rev. Lett., 63, 16
Hummer, D. G., & Mihalas, D. 1988, ApJ, 331, 794
Iben, I., Kalata, K., & Schwartz, J. 1967, ApJ, 150, 1001 (IKS)
Imhof, W. L., et al. 1959, Phys. Rev., 114, 1037
Jackson, J. D. 1975, Classical Electrodynamics, 2nd Ed. (New York: Wiley).
Kavanagh, R. W. 1960, Nucl. Phys., 15, 411
———. 1972, in Cosmology, Fusion, and Other Matters, ed. F. Reines (Boulder: Colorado Associated Univ. Press), 169
Kavanagh, R. W., Tombrello, T. A., Mosher, J. M., & Goosman, D. R. 1969, Bull. Am. Phys. Soc., 14, 1209 (Kav69)
Kolbe, E., Langanke, K., & Assenbaum, H. J. 1988, Phys. Lett., 214, 169
Landau, L. D., & Lifshitz, E. M. 1980, Statistical Physics Part 1 (Oxford: Pergamon)
Lynn, J. E., Jurney, E. T., & Raman, S. 1991, Phys. Rev., C 44, 764
Parker, P. D. 1966, Phys. Rev., 150, 851
———. 1968, ApJ, 153, L85
———. 1986, in Physics of the Sun, Vol. I, ed. P. A. Sturrock, T. E. Holzer, D. M. Mihalas, & R. K. Ulrich (Dordrecht: Reidel), 15
Particle Data Group 1990, Phys. Lett. A, 239, 1
Robertson, R. G. H. 1973, Phys. Rev. C, 7, 543
Rogers, F. J., Graboske, H.C., Jr., & Harwood, D. J. 1970, Phys. Rev. A, 1, 1577
Shen, P. N., Tang, Y. N., Fujiwara, Y., & Kanada, H. 1985, Phys. Rev. C, 31, 2001
Skupsky, S. 1980, Phys. Rev. A, 21, 1316
Theimer, O, & Kepple, P. 1970, Phys. Rev. A, 1, 957
Tombrello, T. A. 1965, Nucl. Phys., 71, 459
Turck-Chièze, S., Cahen, S., Cassé, M., & Doom, C. 1988, ApJ, 335, 415
Wildermuth, K., & Tang, Y. C. 1977, A Unified Theory of the Nucleus (Braunschweig: Vieweg)
Wiezorek, C., Kräwinkel, H., Santo, R., & Wallek, K. 1977, Z. Phys., A, 282, 121
Williams, R. D., & Koonin, S. E. 1981, Phys. Rev. C, 23, 2773
Vaughn, F. J., Chalmers, R. A., Kohler, D., & Chase, L. F., Jr. 1970, Phys. Rev. C, 2, 1657